# Scalar transport modeling for two-phase flows with a diffuse-interface method

**By S. S. Jain AND A. Mani**

## 1. Motivation and objectives

Transport of scalars in a two-phase flow is an interesting problem that finds applications in nature such as environmental processes in the oceans (Craig *et al.* 1993), as well as industrial processes such as electrochemical systems (Fernandez *et al.* 2014), and systems involving cavitation and boiling (Wasekar & Manglik 2000). Typically, this problem involves very disparate length, and time scales and the scalar quantities often experience very large and small diffusivities and mobilities in different phases. These disparate properties result in scalars effectively being confined to one of the phases in the time scales of interest. Hence, it is a numerically challenging task to resolve the gradient of the scalar concentration at the material interface, and it usually leads to numerical leakage and negative values of the scalar concentration at the material interfaces.

To the best of our knowledge, still lacking are numerical methods with simulation capabilities that can accurately capture the behavior of the scalar concentration fields without any numerical leakage from one phase to the other while still maintaining the positivity of the scalar concentration values. To address this deficiency, we have developed a general scalar transport model for two-phase flows, particularly for material interfaces modeled using a diffuse-interface method (phase-field method). Our newly developed scalar transport model prevents the numerical leakage of scalars from one phase to the other, even in challenging flow environments, such as in the presence of electrokinetic effects, and in turbulent flows. We discretize the equation using the second-order central scheme in space due to its non-dissipative nature that is crucial for the simulation of turbulent flows (Mittal & Moin 1997), and we have proved that the resulting discrete equations maintain the positivity of the scalar concentration, given that the parameters in the equation are chosen based on the criterion provided.

The model is general enough that the scalar can represent soluble surfactants, electrolytes, chemical species in combustion modeling, etc. In this article, a generic scalar transport model along with the definition of the scalar concentration will be provided in Section 3. The proposed scalar transport model that is solved in conjunction with the conservative diffuse-interface method (Section 2) will be presented in Section 4. The positivity criterion for the proposed model will be presented in Section 5. Later, the proposed model will be applied towards the simulation of aqueous electrolytes by coupling the scalar transport model, which can be thought of as a modified Nernst-Planck equation (Kirby 2010) for two-phase flows, with the conservative diffuse-interface method (Mirjalili *et al.* 2020; Jain *et al.* 2019), the Navier-Stokes equations and the Maxwell's equations (Griffiths 2005) in Section 6. Finally, we describe the choice of numerical discretization in Section 7 and present our results in Section 8.

## 2. Conservative diffuse-interface method

The first step towards simulating scalars in a two-phase flow is to choose an interface-capturing method that can accurately simulate interfaces in complex flows. In this work, we choose the recently developed conservative diffuse-interface method by Mirjalili *et al.* (2020) (for incompressible flows) and Jain *et al.* (2019) (for compressible flows). In this method, the volume-fraction advection equation is written as

$$\frac{\partial \phi}{\partial t} + (\vec{u} \cdot \vec{\nabla})\phi = \vec{\nabla} \cdot \Big[\Gamma\Big\{\epsilon \vec{\nabla}\phi - \phi(1-\phi)\vec{n}\Big\}\Big], \tag{2.1}$$

where $\phi$ is the volume fraction field, $\Gamma\{\epsilon\vec{\nabla}\phi - \phi(1-\phi)\vec{n}\} = \vec{a}(\phi)$ term on the right-hand side is the flux of the interface regularization (diffusion-sharpening) term, $\vec{n} = \vec{\nabla}\phi/|\vec{\nabla}\phi|$ is the outward normal of the interface, and $\Gamma$ and $\epsilon$ are the interface parameters, where $\Gamma$ represents an artificial regularization velocity scale and $\epsilon$ represents an interface thickness scale. This equation satisfies both $\phi_1$ and $\phi_2$, where $\phi_1$ and $\phi_2 = 1 - \phi_1$ are the volume fraction fields for two phases 1 and 2. We can show that the interface regularization term satisfies $\vec{a}(\phi_1) = -\vec{a}(\phi_2)$ for phases 1 and 2. The volume fraction field $\phi$ is said to be bounded and total-variation diminishing (TVD) if $\Gamma$ and $\epsilon$ are chosen such that they satisfy the criterion

$$\frac{\epsilon}{\Delta x} \geq \frac{(\frac{|u|_{\max}}{\Gamma} + 1)}{2}, \tag{2.2}$$

where $\Delta x$ is the grid size and $|u|_{\max}$ is the maximum value of the velocity in the domain.

Now, making an assumption that the flow is incompressible, Eq. (2.1) reduces to a conservative form of the transport equation

$$\frac{\partial \phi}{\partial t} + \vec{\nabla} \cdot (\vec{u}\phi) = \vec{\nabla} \cdot \Big[\Gamma\Big\{\epsilon \vec{\nabla}\phi - \phi(1-\phi)\vec{n}\Big\}\Big], \tag{2.3}$$

and can be solved in conjunction with the momentum balance equation

$$\frac{\partial \rho\vec{u}}{\partial t} + \vec{\nabla} \cdot (\rho\vec{u} \otimes \vec{u} + p\mathbb{1}) = \vec{\nabla} \cdot \underline{\underline{\tau}} + \vec{\nabla} \cdot (\vec{f} \otimes \vec{u}), \tag{2.4}$$

where $\vec{f} = \sum_{l=1}^{2} \rho_l \vec{a}_l$ is the net mass regularization flux, $\rho_l$ is the density of the phase $l$, and $\rho = \sum_{l=1}^{2} \rho_l \phi_l$ is the total density of the mixture. The Cauchy stress tensor is written as $\underline{\underline{\tau}} = 2\mu\mathbb{D} - 2\mu(\vec{\nabla} \cdot \vec{u})\mathbb{1}/3$, where $\mu$ is the dynamic viscosity of the mixture evaluated using the one-fluid mixture rule (Kataoka 1986) as $\mu = \sum_{l=1}^{2} \phi_l \mu_l$, $\mathbb{D} = \{(\vec{\nabla}\vec{u}) + (\vec{\nabla}\vec{u})^T\}/2$ is the strain-rate tensor, and $p$ is the pressure. Since an incompressible flow assumption is made, a pressure field $p$ that satisfies the criterion of zero velocity divergence can be computed using the fractional-step method of Kim & Moin (1985) adapted for two-phase flows.

The advantages of this diffuse-interface method are that it maintains the boundedness of the volume fraction field even with the use of a central-difference scheme for the discretization of all the operators, which is a physical realizability requirement for the simulation of two-phase flows. The transport of the volume fraction field also inherently satisfies the TVD property without having to add any flux limiters that destroy the non-dissipative nature of the scheme. Another advantage of all diffuse-interface methods is that the absence of geometric reconstruction of the interface (typical of sharp-interface methods) results in a low-cost, load-balanced, and highly scalable method; see Jain *et al.* (2019) for the scalability tests. For more discussion and comparison between sharp-interface and diffuse-interface methods, see Mirjalili *et al.* (2017, 2019).

## 3. Transport equation for scalar

Let $c$ represent the local concentration (amount of scalar per unit volume) of any scalar quantity of interest. If the scalar quantity is not being generated or destroyed, then it is conserved, implying that

$$\int_{\Omega} c \, dV = \text{constant}, \tag{3.1}$$

where $\Omega$ is the domain. If the scalar is now confined to only one of the phases, we can then define another variable $\tilde{c}$ that represents the local concentration of the scalar in that phase (amount of scalar per unit volume of the phase). Then, the relation between $c$ and $\tilde{c}$ is

$$c = \phi\tilde{c}, \tag{3.2}$$

where $\phi$ represents the volume fraction of the phase (volume of the phase per total volume) where the scalar is present. In the limit of the interface being infinitely sharp, $\phi$ reduces to a Heaviside function that is 1 inside the phase and 0 outside. Hence, in the infinitely sharp interface limit

$$c = \begin{cases} \tilde{c} & \text{inside the phase where scalar is present} \\ 0 & \text{elsewhere.} \end{cases} \tag{3.3}$$

Now, assuming that $\tilde{c}$ satisfies a generic transport (advection-diffusion) equation within the phase

$$\frac{\partial\tilde{c}}{\partial t} + \vec{\nabla}\cdot(\vec{u}_c\tilde{c}) = \vec{\nabla}\cdot(D\vec{\nabla}\tilde{c}), \tag{3.4}$$

where $\vec{u}_c = \vec{u} + \vec{u}_r$ represents the total convective velocity of the scalar, $\vec{u}$ represents the fluid velocity, $\vec{u}_r$ represents any effective velocity with which the scalar is being advected relative to the fluid (e.g., electromigration velocity $\vec{u}_r = \nu\vec{E}$, where $\nu$ is the electrical mobility and $\vec{E}$ is the electric field), and $D$ represents the diffusivity of the scalar. Since the scalar is confined to the phase and is not allowed to cross the phase boundary, the no-flux boundary condition can be written as

$$(D\nabla\tilde{c} - \vec{u}_r\tilde{c})\cdot\vec{n} = 0. \tag{3.5}$$

Combining Eq. (3.4) and Eq. (3.5), we can arrive at the form

$$\frac{\partial(\phi\tilde{c})}{\partial t} + \vec{\nabla}\cdot(\phi\vec{u}_c\tilde{c}) = \vec{\nabla}\cdot(D\phi\vec{\nabla}\tilde{c}). \tag{3.6}$$

A similar form of the equation was used by Berry *et al.* (2013) along with a sharp-interface method (coupled level-set and volume-of-fluid method) to simulate the electrokinetics of liquid-liquid systems.

In the discrete limit, however, the interface is not infinitely sharp, and the smallest interface thickness that can be handled on an Eulerian grid is $\sim \mathcal{O}(\Delta x)$. The discrete representation of $c$ and $\tilde{c}$ are shown in Figure 1. In this discrete limit that is typical of all numerical simulations, we can observe that $\tilde{c}$ is not a conserved quantity and it does not satisfy the transport equation in Eq. (3.4), unless an equivalent discrete implementation is derived. However, $c$ is still a conserved quantity [Eq. (3.1)], and hence we could instead write a transport equation for $c$ and look for modifications that mimic the no-flux boundary condition at the interface. In other words, the profile of the scalar concentration field $c$ must be consistent with the profile of the volume fraction field $\phi$ at the interface (see Figure 3; we define consistency more rigorously in Section 4.1). With

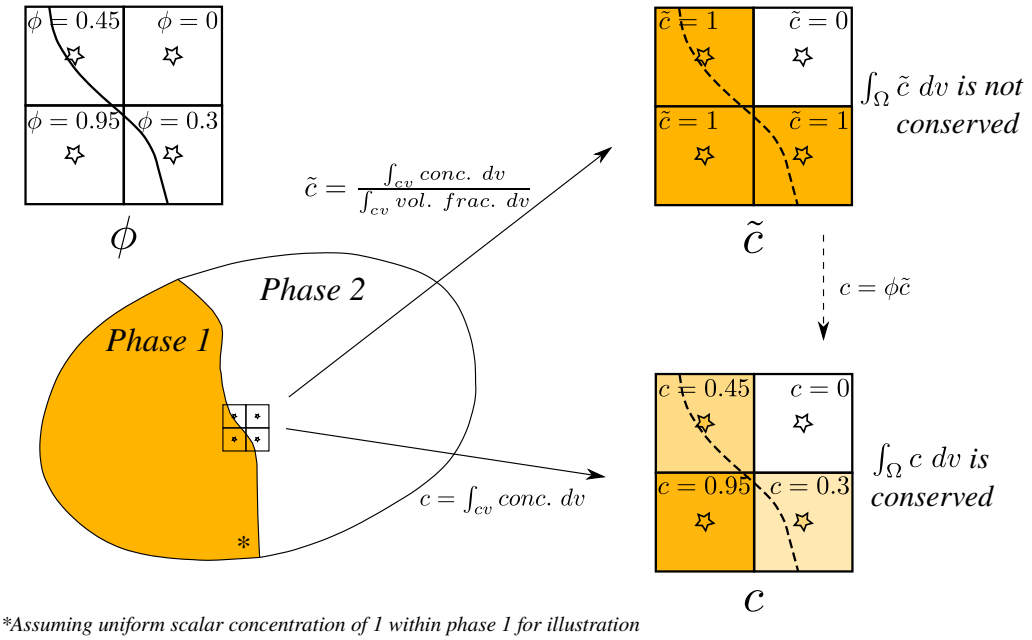


FIGURE 1. Schematic representing the discrete $c$ and $\tilde{c}$ quantities. Opacity of the color is proportional to the field value in that particular cell. Here, "conc." represents the local scalar concentration, "vol. frac." is the local volume fraction of the phase and $cv$ represents a control volume.

this notion, we could start with a generic form of the transport equation for $c$ as

$$\frac{\partial c}{\partial t} + \vec{\nabla} \cdot (\vec{u}_c c) = \vec{\nabla} \cdot (D\vec{\nabla} c). \tag{3.7}$$

A straightforward modification (a naive approach) to this equation could be to multiply $\phi$ to $\vec{u}_r$ and $D$, such that the flux $D\vec{\nabla}c - \vec{u}_r c$ goes to zero as $\phi$ goes to zero outside the phase as

$$\frac{\partial c}{\partial t} + \vec{\nabla} \cdot (\vec{u}c + \phi\vec{u}_r c) = \vec{\nabla} \cdot (D\phi\vec{\nabla} c). \tag{3.8}$$

Though this simple modification to achieve no-flux boundary condition sounds promising, the scalar concentration field $c$ that we obtain by solving Eq. (3.8) will not be consistent with the volume fraction field $\phi$, and in the long run, it results in predicting a lower value of $c$ with an $\mathcal{O}(1)$ error due to the numerical leakage of scalar as shown in Figure 2, thus affecting the overall accuracy of the solution. In problems with two-way coupling between the flow and the transport of scalar, the local concentration of the scalar field is crucial in predicting accurate flow fields. For example, the transport of reacting species in combustion modeling and ion transport in electrokinetics both modify the flow field depending on the local concentration of the scalar being transported, and the spurious leakage of the scalar and the resulting $\mathcal{O}(1)$ error could be detrimental to the overall accuracy of the simulation. In the worst case scenario, the numerical solution for the scalar concentration field can admit unphysical negative values near the interface and often within the phase with lower diffusivity, which might result in unrealizable scalar concentration fields.

Common ways to address this issue of unphysical negative values is to use flux limiters

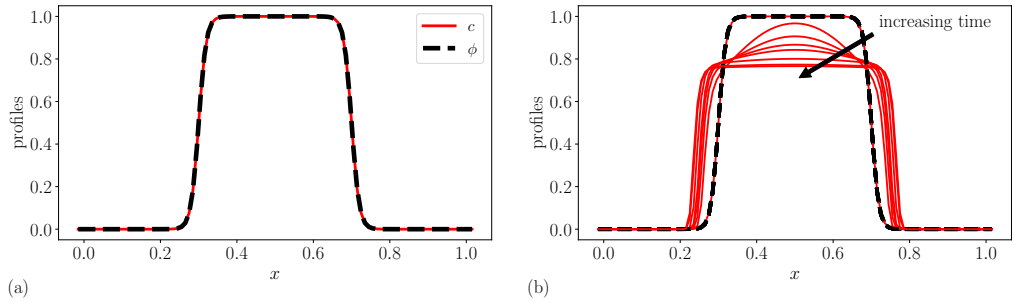


FIGURE 2. Simulation results obtained by solving Eq. (3.8), showing the one-dimensional drop ($\phi$ field) and the scalar concentration ($c$ field) at (a) initial time and (b) later times. Parameters used in this simulation are $D = 0.01$, $\Delta x = 0.01$, $u = 0$, and $u_r = 0$. The arrow denotes the time evolution of the scalar concentration field.

and positivity-preserving limiters (Laney 1998). However, the numerical diffusivity associated with these schemes inevitably adds to the unphysical leakage of the scalar across the interface and into the impermeable phase. Hence, in the current work, we present a modified equation for the transport of scalars in two-phase flows, along with a consistent numerical discretization scheme that overcomes the challenges that were presented here.

## 4. Proposed model equation for scalar transport in two-phase flows

With the objective of developing a scalar transport model that does not admit negative values for the scalar concentration field, nor permit unphysical leakage of the scalar across the interface, we propose a model of the form

$$\frac{\partial c}{\partial t} + \vec{\nabla} \cdot (\vec{u}c + \phi \vec{u}_r c) = \vec{\nabla} \cdot \left[ D \left\{ \vec{\nabla} c - \frac{(1-\phi)\vec{n}c}{\epsilon} \right\} \right], \tag{4.1}$$

where $\vec{n}$ is the outward normal vector to the phase where the scalar is assumed to be present, $\epsilon$ is the same interface parameter that is present in Eqs. (2.1)-(2.3). The proposed model equation in Eq. (4.1) is a modification to Eq. (3.8), which failed to prevent numerical leakage of the scalar and maintain the no-flux boundary condition for the scalar at the interface (Figure 2). The proposed model equation in Eq. (4.1) is valid for both incompressible and compressible flows. However, in this brief, the focus will be on the incompressible regime.

Away from the interface, in the bulk region where the scalar is assumed to be present ($\phi \to 1$), the proposed model in Eq. (4.1) reduces to

$$\frac{\partial c}{\partial t} + \vec{\nabla} \cdot (\vec{u}c + \vec{u}_r c) = \vec{\nabla} \cdot \left( D \vec{\nabla} c \right), \tag{4.2}$$

which is a generic transport equation (advection-diffusion) for scalars in the bulk region. Hence, the model has no effect on the transport of scalars away from the interface.

### 4.1. *Equilibrium solutions*

As described in Section 3, consistency of the scalar concentration field $c$ and the volume fraction field $\phi$ is crucial in preventing the unphysical numerical leakage of the scalar across the interface, when the scalar is confined to only one of the phases. To present this consistency of the scalar concentration field obtained by solving the proposed model in

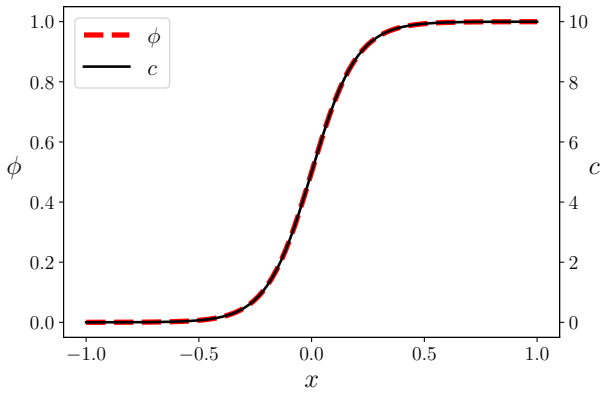


FIGURE 3. Equilibrium solutions for $\phi$ and $c$, showing consistency between the scalar concentration field and the volume fraction field. Here, $c_0$ is chosen to be equal to 5 for illustration.

Eq. (4.1) and the volume fraction field obtained by solving the diffuse-interface model in Eq. (2.1), we look at the steady-state equilibrium solutions to the corresponding equations. In steady state, for $\vec{u} = 0$ and $\vec{u}_r = 0$ and in one dimension, the volume-fraction advection equation in Eq. (2.1) reduces to the form

$$0 = \vec{\nabla} \cdot \left[ \Gamma\epsilon \left\{ \vec{\nabla}\phi - \frac{(1-\phi)\vec{n}\phi}{\epsilon} \right\} \right] \Rightarrow \frac{d^2\phi}{dx^2} - \frac{1}{\epsilon}\frac{d\{(1-\phi)\phi\}}{dx} = 0, \tag{4.3}$$

for $\vec{n} = +1$ and the proposed scalar-transport equation in Eq. (4.1) reduces to the form

$$0 = \vec{\nabla} \cdot \left[ D \left\{ \vec{\nabla}c - \frac{(1-\phi)\vec{n}c}{\epsilon} \right\} \right] \Rightarrow \frac{d^2c}{dx^2} - \frac{1}{\epsilon}\frac{d\{(1-\phi)c\}}{dx} = 0. \tag{4.4}$$

Now, assuming that the interface is at the origin as shown in Figure 3, and integrating the Eq. 4.3 along with the boundary conditions

$$\phi = \begin{cases} 0 & x \to -\infty \\ 0.5 & x = 0, \end{cases} \tag{4.5}$$

we obtain

$$\phi = \frac{e^{(x/\epsilon)}}{1 + e^{(x/\epsilon)}} = \frac{1}{2}\left\{ 1 + \tanh\left( \frac{x}{2\epsilon} \right) \right\}. \tag{4.6}$$

Using the equilibrium solution for $\phi$ in Eq. (4.6) and solving for $c$ by integrating the Eq. (4.4) and using the boundary conditions

$$c = \begin{cases} 0 & x \to -\infty \\ c_0 & x = 0, \end{cases} \tag{4.7}$$

we obtain

$$c = 2c_0 \frac{e^{(x/\epsilon)}}{1 + e^{(x/\epsilon)}} = c_0 \left\{ 1 + \tanh\left( \frac{x}{2\epsilon} \right) \right\}. \tag{4.8}$$

Hence, the equilibrium profiles of $c$ and $\phi$ are both a hyperbolic tangent functions of the spatial coordinate $x$, and are consistent at the interface, which represents a constant $\tilde{c}$ (see Figure 1). If we choose $c_0$ to be equal to 0.5, the $c$ and $\phi$ profiles are identical. For other values of $c_0$, $c$ is only scaled by a constant factor, but still retains a hyperbolic

tangent shape as illustrated in Figure 3. Here, $c_0$ was chosen to be equal to 5, for the sake of illustration. Hence, the scalar concentration and volume fraction fields are consistent, which results in the transport of scalar within the phase with an effective no-flux boundary condition at the interface.

## 5. Positivity of scalars

Positivity of the scalar concentration field is a crucial realizability criterion that needs to be satisfied at all times in the simulation. A common approach to achieve this is to use flux limiters and positivity-preserving limiters (Laney 1998). However, these limiters add artificial dissipation to the scheme and also lead to unphysical leakage of the scalar across the interface. Hence, we use a central-difference scheme to discretize the operators in our system of equations because of its well-known non-dissipative property (Moin & Verzicco 2016), and derive a criterion [Eq. (5.1); Figure 4] for the choice of grid size to be used in the simulation. We propose in Theorem 5.1 that the criterion in Eq. (5.1) is a sufficient condition for the proposed model transport equation in Eq. (4.1) to maintain the positivity of scalar concentration field $c$ at all times during the simulation.

THEOREM 5.1. *If $\phi^k$ is bounded between 0 and 1 $\forall k \in \mathbb{Z}^+$ on a uniform one-dimensional grid, then $c_i^k \geq 0$ holds $\forall k \in \mathbb{Z}^+$, where $k$ is the time-step index and $i$ is the grid index, provided*

$$\Delta x \leq \left( \frac{2D}{|u|_{\max} + |u_r|_{\max} + \frac{D}{\epsilon}} \right), \tag{5.1}$$

*where $|u|_{\max}$ and $|u_r|_{\max}$ are the maximum fluid velocity and relative velocity of the scalar in the domain, and*

$$\Delta t \leq \frac{\Delta x^2}{2D} \tag{5.2}$$

*are satisfied.*

Proof of Theorem 5.1 is deferred to a future article. Note that $\phi$ is assumed to be bounded throughout the simulation. This boundedness of $\phi$ can be achieved by choosing appropriate values for the interface parameters $\Gamma$ and $\epsilon$ such that they satisfy the criterion in the Eq. (2.2). For more details on the boundedness of $\phi$, see Mirjalili *et al.* (2020) for incompressible flows and Jain *et al.* (2019) for compressible flows.

The criterion on the time-step size in the Eq. (5.2) is a Courant-Friedrich-Levy (CFL) condition for the scalar diffusion process, and is typically already satisfied in an explicit time-marching scheme to achieve temporal stability. Hence, the only additional criterion that needs to be satisfied to maintain the positivity of the evolution of the scalar concentration field is the restriction on the grid size given in the Eq. (5.1).

It was shown in Section 4 that the proposed model transport equation in Eq. (4.1) reduces to a generic transport equation [Eq. (4.2)] for scalars in the bulk region away from the interface. Now, repeating the analysis in Theorem 5.1 for the scalar transport equation for the bulk region [Eq. (4.2)], we can show that the criterion that needs to be satisfied to maintain the positivity of evolution of the scalar concentration field is the restriction on the grid size given by

$$\Delta x \leq \left( \frac{2D}{|u|_{\max} + |u_r|_{\max}} \right). \tag{5.3}$$

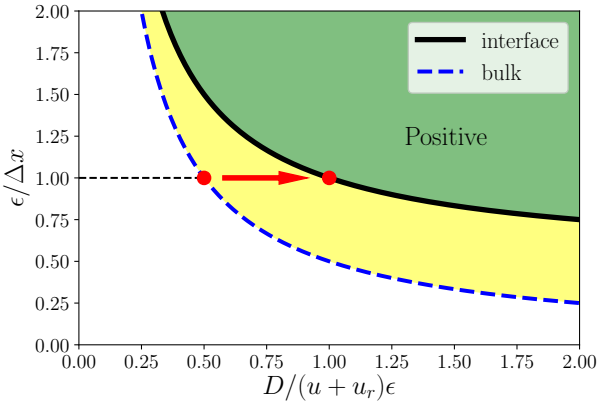


FIGURE 4. Graphical representation of the positivity criteria. The solid line is the positivity criterion in Eq. (5.4) for the proposed scalar transport model [Eq. (4.1)], and the dashed line is the positivity criterion in Eq. (5.5) for the reduced scalar transport model for the bulk region away from the interface [Eq. (4.2)]. The dots represent the positivity criteria for the choice of $\epsilon = \Delta x$ and the arrow represents the additional restriction imposed on the grid size due to the effective no-flux boundary condition for the scalar at the interface compared to the bulk region away from the interface.

### 5.1. *Spatial resolution requirements*

Now, rewriting the positivity criterion for the proposed scalar transport model in Eq. (5.1) in terms of the non-dimensional groups $[\epsilon/\Delta x]$ and $[D/\{(u+u_r)\epsilon\}]$ as

$$\left[\frac{\epsilon}{\Delta x}\right] \geq \frac{1+\left[\frac{D}{(u+u_r)\epsilon}\right]}{2\left[\frac{D}{(u+u_r)\epsilon}\right]} \tag{5.4}$$

and the positivity criterion in Eq. (5.3) for the bulk region away from the interface as

$$\left[\frac{\epsilon}{\Delta x}\right] \geq \frac{1}{2\left[\frac{D}{(u+u_r)\epsilon}\right]}, \tag{5.5}$$

where $u = |u|_{max}$ and $u_r = |u_r|_{max}$, symbol $[\cdot]$ represents a non-dimensional group. By plotting $[\epsilon/\Delta x]$ vs $[D/\{(u+u_r)\epsilon\}]$ in Figure 4, we can see that any grid size $\Delta x$ for a given $\epsilon$ and $D$ that lies above the lines maintains the positivity of the scalar concentration field throughout the simulation. The solid line in Figure 4 is for the proposed model transport equation in Eq. (4.1) and the dashed line is for the reduced transport equation in Eq. (4.2) for the bulk region away from the interface. Because the proposed model transport equation imposes a more restrictive condition on the grid size $\Delta x$ for a given $\epsilon$ and $D$ than the reduced transport equation, the criterion in Eq. (5.1) should be used to choose the grid size throughout the domain.

In the conservative diffuse-interface method, $\epsilon$ is typically chosen to be equal to $\Delta x$ (Jain *et al.* 2019). With this choice of $\epsilon$, and recognizing that the non-dimensional group $[D/\{(u+u_r)\epsilon\}] = [D/\{(u+u_r)\Delta x\}]$ is the inverse of Peclet number ($Pe$), the positivity

criterion for the proposed model in Eq. (5.1) reduces to

$$1 \geq \frac{1 + \left[\frac{1}{Pe_I}\right]}{2\left[\frac{1}{Pe_I}\right]} \Rightarrow Pe_I \leq 1, \tag{5.6}$$

where the subscript $I$ in $Pe_I$ is used to denote that the criterion is for the region at the material interface, and the positivity criterion in Eq. (5.3) for the bulk region away from the interface reduces to

$$1 \geq \frac{1}{2\left[\frac{1}{Pe_B}\right]} \Rightarrow Pe_B \leq 2, \tag{5.7}$$

where the subscript $B$ in $Pe_B$ is used to denote that the criterion is for the bulk region. This criterion is consistent with the boundedness criterion ($Pe \leq 2$) for a generic scalar transport equation first proposed by Patankar (1980) and Versteeg & Malalasekera (2007). Hence, the presence of a material interface and the effective no-flux boundary condition for the scalar at the interface has introduced an additional restriction in terms of the cell Peclet number ($Pe_I \leq 1$), which otherwise would have been $Pe_B \leq 2$ in the absence of any interface, which is also graphically shown (arrow) in Figure 4. Therefore, assuming a uniform grid throughout the domain, the grid size for the simulation of scalars with material interfaces (two-phase flow) should be twice as small compared to the grid size for the simulation of scalars in the absence of material interfaces (single-phase flow).

## 6. Modeling electrokinetics in two-phase flow systems

In this section, the proposed scalar transport equation will be recast into a modified Nernst-Planck equation that can be used for the simulation of ion transport in two-phase media. If $c^+$ and $c^-$ represent the cationic and anionic concentration fields, respectively; $D^+$ and $D^-$ represent the cationic and anionic diffusion coefficients, respectively; and $\vec{u}_r$ the electromigration velocity $\vec{u}_r = \nu\vec{E}$, where $\nu$ is the electrical mobility and $\vec{E}$ is the electric field; then the proposed scalar transport model in Eq. (4.1) can be written as a modified Nernst-Planck equation

$$\frac{\partial c^\pm}{\partial t} + \vec{\nabla}\cdot(\vec{u}c^\pm \pm \phi\nu\vec{E}c^\pm) = \vec{\nabla}\cdot\left[D^\pm\left\{\vec{\nabla}c^\pm - \frac{(1-\phi)\vec{n}c^\pm}{\epsilon}\right\}\right]. \tag{6.1}$$

Combining this equation with the Gauss's law

$$\vec{\nabla}\cdot(\varepsilon\vec{E}) = \rho^f, \tag{6.2}$$

where $\rho^f = z^+ec^+ - z^-ec^-$ is the free charge density; $z^+$ and $z^-$ represent the cationic and anionic valences, respectively; $e$ is the elementary charge; and $\varepsilon$ is the electrical permittivity of the electrolyte. Making an electrostatic approximation, i.e., assuming that the time variation of the magnetic field is much slower compared to that of the electric field, the electric field can be shown to be irrotational using Faraday's law (Griffiths 2005). Hence it can be written as

$$\vec{E} = -\vec{\nabla}\psi, \tag{6.3}$$

where $\psi$ is the electrostatic potential. Electrostatic phenomena and hydrodynamics are coupled through the Maxwell stress tensor (Saville 1997), and the electrohydrodynamic force on the fluid can be written as $\rho^f\vec{E} - (\vec{E}\cdot\vec{E})\vec{\nabla}\varepsilon/2$. Thus, rewriting the volume fraction advection equation in Eq. (2.3), momentum balance equation in Eq. (2.4) with

the electrohydrodynamic force, continuity equation, Nernst-Planck equation in Eq. (6.1) and Gauss's law in Eq. (6.2) along with the electrostatic approximation in Eq. (6.3), the system of equations that models the transport of charged ionic species in two-phase flows with incompressible Newtonian immiscible fluids can be written as

$$\begin{gathered}
\frac{\partial \phi}{\partial t} + \vec{\nabla} \cdot (\vec{u}\phi) = \vec{\nabla} \cdot \left[\Gamma \left\{ \epsilon \vec{\nabla}\phi - \phi(1-\phi)\vec{n} \right\}\right], \\
\frac{\partial \rho \vec{u}}{\partial t} + \vec{\nabla} \cdot (\rho \vec{u} \otimes \vec{u} + p\mathbb{1}) = \vec{\nabla} \cdot \underline{\underline{\tau}} + \vec{\nabla} \cdot (\vec{f} \otimes \vec{u}) - \rho^f \vec{\nabla}\psi - \frac{1}{2}(\vec{\nabla}\psi \cdot \vec{\nabla}\psi)\vec{\nabla}\varepsilon, \\
\vec{\nabla} \cdot \vec{u} = 0, \\
\frac{\partial c^{\pm}}{\partial t} + \vec{\nabla} \cdot \left\{ \vec{u}c^{\pm} \mp \phi\nu(\vec{\nabla}\psi)c^{\pm} \right\} = \vec{\nabla} \cdot \left[ D^{\pm} \left\{ \vec{\nabla}c^{\pm} - \frac{(1-\phi)\vec{n}c^{\pm}}{\epsilon} \right\} \right], \\
-\vec{\nabla} \cdot \left(\varepsilon \vec{\nabla}\psi\right) = \rho^f .
\end{gathered} \tag{6.4}$$

## 7. Numerical discretization

In this work, we use the fourth-order Runge-Kutta (RK4) time-stepping scheme and second-order central-differencing scheme for the discretization of all spatial operators. This choice of numerical scheme has some advantages, particularly for the simulation of turbulent flows due to its (a) non-dissipative nature, (b) low aliasing error, (c) easy boundary treatment, (d) low cost, and (e) improved stability (Moin & Verzicco 2016). With the appropriate choice of $\Delta x$, $\Gamma$, and $\epsilon$, we can achieve the positivity for the scalar concentration field (Section 5), and boundedness and TVD properties for the volume fraction field (Section 2) even with the use of a central-difference scheme for all the spatial operators which would otherwise admit oscillatory solutions due to the associated dispersion errors.

A finite-volume staggered discretization strategy has been employed wherein $\phi$, $p$, $\psi$, and $c^{\pm}$ are stored at cell centers, and components of $\vec{u}$ are stored at the cell faces where all the fluxes are evaluated. This choice of discretization is to avoid the spurious checkerboarding of the pressure field in incompressible flows (Patankar 1980).

## 8. Results

In this section, multiple verification tests are presented that are used to assess the newly proposed model, the numerical discretization, and the implementation. The verification tests used in this work can be broadly classified into (a) positivity test cases, that test the positivity of the scalar concentration field for various choices of parameters in the positivity map (Figure 4) to test the validity of the positivity criterion. These test cases also evaluate the effective no-flux boundary condition for the scalar at the interface, with and without the relative velocity of the scalar with respect to the fluid; (b) charge-in-a-drop test, that evaluates the no-flux boundary condition for the charged ions when the Nernst-Planck equation is coupled with Gauss's law and hydrodynamics.

### 8.1. *Positivity test*

In this test case, four different choices of parameters are made as shown in Figure 5(a) in terms of the Peclet number ($Pe = (u+u_r)\Delta x/D$), such that two of the four choices ($Pe = 1, 0.8$) satisfy the positivity criterion in Eq. (5.6) and the other two ($Pe = 2, 4$) violate the criterion. To test this validity of the positivity criterion, a one-dimensional domain of

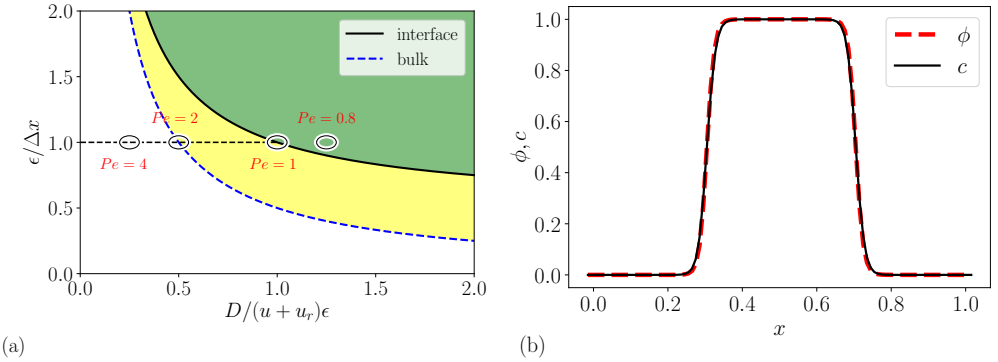


FIGURE 5. (a) Four different choices of parameters to test the validity of the positivity criterion. (b) Initial condition for the volume fraction field $\phi$ and the scalar concentration field $c$ for the positivity tests.

range $[0, 1]$ is chosen with periodic boundary conditions. The domain is discretized into a uniform grid of size $\Delta x = 0.01$. A drop of radius $R = 0.25$ is initially placed in the domain centered at $x_0 = 0.5$, with a uniform scalar concentration of 1 inside the drop and 0 outside as shown in Figure 5(b). Interface parameters are chosen as $\Gamma = 100$ and $\epsilon = \Delta x$. This test case is repeated for zero and non-zero relative velocity for the scalar with respect to the fluid, as further described in the subsequent Sections 8.1.1 and 8.1.2.

### 8.1.1. *No relative velocity ($\vec{u}_r = 0$)*

Here, the uniform fluid velocity is chosen to be $\vec{u} = 100$, the relative velocity of the scalar with respect to the fluid is $\vec{u}_r = 0$ and the total integration time is $t_{\text{end}} = 10$. The diffusivity of the scalar is chosen based on the required Peclet number. The drop advects to the right due to the imposed fluid velocity and returns to its original position at $t = 0.01$ due to the periodic boundary condition, and this process repeats 1000 times until the time $t = 10$. The final state of the drop and the scalar concentration field at time $t = 10$ is shown in Figure 6 along with the minimum value of the scalar concentration for all four choices of parameters shown in Figure 5. Clearly, for cases with $Pe = 1$ and 0.8 that satisfy the positivity criterion in Eq. (5.6), the scalar concentration $c$ is positive throughout the domain, and for cases with $Pe = 2$ and 4 that violate the positivity criterion, the scalar concentration $c$ admits negative values close to the interface, as expected, which verifies the proposed scalar transport model and the positivity criterion. Comparing the results in Figure 6 with those in Figure 2, where the scalar was found to leak outside the drop resulting in an $\mathcal{O}(1)$ error of the scalar concentration, it is easy to see the role and importance of the effective no-flux boundary condition embedded in the proposed scalar transport model in Eq.(4.1).

### 8.1.2. *With relative velocity ($\vec{u}_r \neq 0$)*

Here, the uniform fluid velocity is chosen to be $\vec{u} = 50$, the relative velocity of the scalar with respect to the fluid is $\vec{u}_r = 50$, and the total integration time is $t_{\text{end}} = 10$. The diffusivity of the scalar is chosen based on the required Peclet number. The drop advects to the right due to the imposed fluid velocity and returns to its original position at $t = 0.02$ due to the periodic boundary condition, and this process repeats 500 times until time $t = 10$. The scalar also advects relative to the drop to the right and accumulates on the right of the drop. It reaches a steady state when the diffusion balances the advection

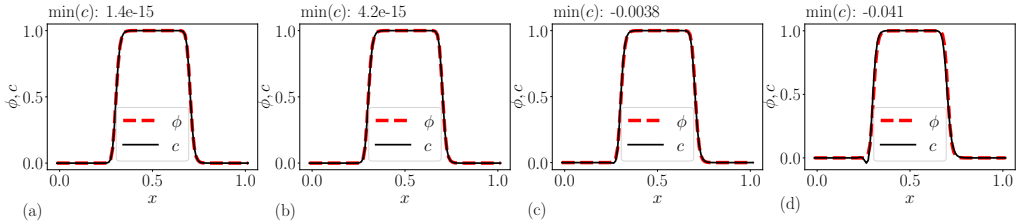


FIGURE 6. Final state of the drop and scalar at time $t = 10$ for (a) $Pe = 1$, (b) $Pe = 0.8$, (c) $Pe = 2$, and (d) $Pe = 4$ with $u_r = 0$.

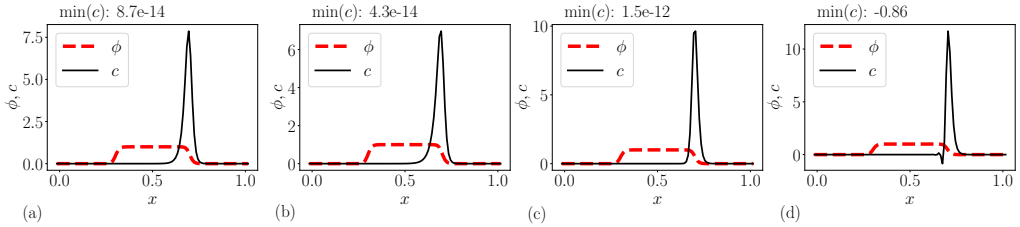


FIGURE 7. Final state of the drop and scalar at time $t = 10$ for (a) $Pe = 1$, (b) $Pe = 0.8$, (c) $Pe = 2$, and (d) $Pe = 4$ with $u_r \neq 0$.

due to the relative velocity. The final state of the drop and the scalar concentration field at time $t = 10$ are shown in Figure 7 along with the minimum value of the scalar concentration for all four choices of parameters shown in the Figure 5. Clearly, for the cases with $Pe = 1$ and 0.8 that satisfy the positivity criterion in Eq. (5.6), the scalar concentration $c$ is positive throughout the domain and for the cases with $Pe = 2$ and 4 that violate the positivity criterion, the scalar concentration $c$ admits negative values for $Pe = 4$, as expected. However the positivity is still maintained for $Pe = 2$ though the criterion is violated. This is because the criterion is only a sufficient, not a necessary condition for the scalar concentration field to remain positive and therefore presents the most restrictive condition such that the positivity of the scalar is satisfied even in some situations when the criterion is violated. This shows the robustness of the positivity criterion that is crucial in maintaining the realizable values of the scalar concentration field throughout the duration of the simulation. This again verifies the positivity criterion for the proposed scalar transport model.

### 8.1.3. *Nonuniform scalar concentration within the drop*

The results up to here all had initial conditions with uniform scalar concentration field within the drop. However, in reality, the scalar concentration can be nonuniform inside the drop. To evaluate the model for this scenario, a one-dimensional domain of range $[0, 5]$ is chosen with periodic boundary conditions. The domain is discretized into a uniform grid of size $\Delta x = 0.01$. A drop of radius $R = 0.25$ is initially centered at $x_0 = 0.5$, with a nonuniform scalar concentration field inside the drop given by the compact support function

$$c = \begin{cases} Ae^{\left\{\frac{1}{(4x-2)^2-1}\right\}} & x \in [0.25, 0.75] \\ 0 & \text{else,} \end{cases} \tag{8.1}$$

as shown in Figure 8(a), where $A$ is a factor chosen to make $\int_\Omega c\, dV$ and $\int_\Omega \phi\, dV$ equal discretely, such that as the scalar diffuses and reaches a steady state within the drop, the

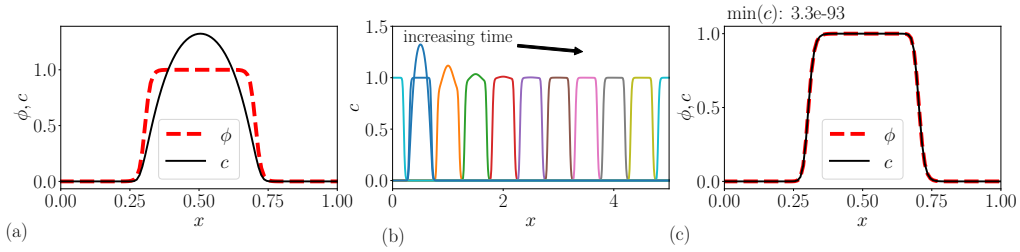


FIGURE 8. The time evolution of the scalar with a nonuniform initial concentration within the drop. (a) Initial conditions for $\phi$ and $c$. (b) The time evolution of $c$. (c) The final states of $\phi$ and $c$.

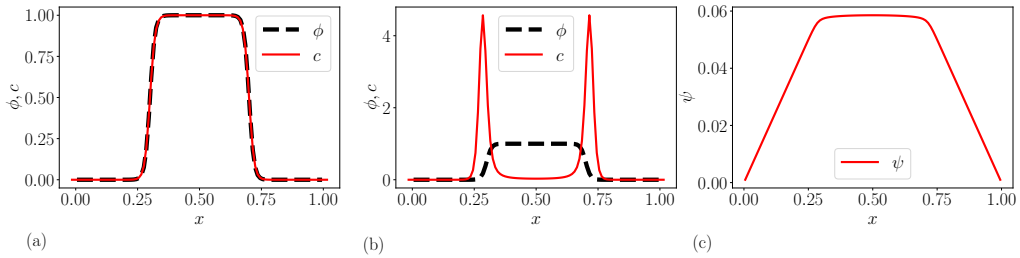


FIGURE 9. Reorganization of the charged ions in a stationary drop. (a) Initial conditions for $\phi$ and $c$. (b) The final states of $\phi$ and $c$. (c) The electrostatic potential in the domain at the final state due to the charge distribution.

scalar concentration reaches a uniform value of 1 within the drop. Interface parameters are chosen as $\Gamma = 100$ and $\epsilon = \Delta x$. The uniform fluid velocity is chosen to be $\vec{u} = 100$, the relative velocity of the scalar with respect to the fluid is $\vec{u}_r = 0$, and the total integration time is $t_{\text{end}} = 0.05$. The diffusivity of the scalar is chosen such that the Peclet number is 1. Initial conditions for $\phi$ and $c$, the time evolution of $c$, and the final state are shown in Figure 8(a,b,c), respectively. Clearly, the scalar diffuses within the drop without any numerical leakage, and at the final time, the scalar concentration is uniform within the drop as expected, which illustrates the robustness of the proposed model.

### 8.2. *Charge in a drop: one-way coupled case*

In this test case, the system of equations for the volume fraction advection equation, the Nernst-Planck equation, and Gauss's law along with the electrostatic approximation in Eq. (6.4) are solved together to simulate the transport of charged ions in a drop. Hydrodynamics is decoupled from the ion transport to study only the behavior of flow of ions due to unbalanced charge. Only cations are assumed to be present. Here, a one-dimensional domain with range $[0, 1]$ is chosen with periodic boundary conditions. The domain is discretized into a uniform grid of size $\Delta x = 0.01$. A drop of radius $R = 0.25$ is initially centered at $x_0 = 0.5$, with a uniform cation concentration of 1 inside the drop and 0 outside as shown in Figure 9(a). Interface parameters are chosen as $\Gamma = 100$ and $\epsilon = \Delta x$. Here, initially the system is at rest and the simulation is integrated until the steady state. As the system is allowed to evolve, the charged ions migrate to the sides of the drop and accumulate at the interface from an initial uniform distribution due to Coulombic repulsion, thus reducing the potential energy of the system as shown in Figure

9(b). The resulting electrostatic potential in the domain due to the charge redistribution can also be seen in Figure 9(c).

### 8.3. *Charge in a perturbed two-dimensional drop*

In this test case, the full coupled system of equations in Eq. (6.4) are solved together to simulate the transport of cations in a drop that is two-way coupled with the hydrodynamics. Here, a two-dimensional domain of range $[-0.5, 0.5] \times [-0.5, 0.5]$ is chosen with Neumann boundary conditions. The domain is discretized into a uniform grid with $1200^2$ grid points. A circular drop of radius $R = 0.15$ is initially perturbed to form an ellipse with semi-major and semi-minor axes 0.16 and 0.14, respectively, and is centered at $(0, 0)$. The initial setup has a uniform cation concentration of 1 inside the drop and 0 outside. The mobility of the scalar is chosen to be $\nu = 2.5$; the diffusivity as $D = 0.01$; the density of the drop and the surrounding fluid as 10 and 1, respectively; the viscosity of the drop and the surrounding fluid are $8.9 \times 10^{-4}$ and $1.81 \times 10^{-5}$, respectively; and the surface tension between the drop and the surrounding fluid as $\sigma = 1$. Interface parameters are chosen as $\Gamma = |u|_{\max}$ and $\epsilon = \Delta x$. The simulation is run for up to a time of $t_{\text{end}} \approx 0.06$ and snapshots at various time instances are shown in Figure 10.

The ions in the drop start migrating towards the surface of the drop, as can be seen at $t = 0.0125$ due to the electrostatic repulsive forces. Further, the forces exerted by the repelling ions start to deform the drop and deform it into an elongated drop at $t = 0.0375$. Since the drop is assumed to be incompressible, extension of the drop in one direction creates a dimple in the other and therefore the drop cannot undergo a volumetric oscillation mode, which might be seen if it was assumed to be compressible. Later, the drop breaks up into two daughter drops, as can be seen at $t = 0.05371$ along with ligaments and satellite drops.

Further theoretical analysis on the behavior of breakup of a drop due to the addition of ions with unbalanced charge is currently underway and will be in discussed in a future article.

## 9. Conclusions

In this work, we proposed a novel scalar transport model for two-phase flows suitable for the modeling of scalars that are confined to one phase in a two-phase flow. The confinement of the scalar to one phase is due to the disparate values of diffusivity and mobility in the phases, and this typically poses a challenge for any numerical method in resolving the gradient of the scalar at the material interface.

We therefore developed and verified a general scalar transport model for two-phase flows, particularly for interfaces represented using a diffuse-interface method (phase-field method) and showed that our newly proposed model equation prevents any numerical leakage from one phase to the other, while maintaining the positive value for the scalar concentration throughout the simulation, which is a crucial realizability condition for the simulation of scalars.

Finally, we recast the proposed scalar transport model for two-phase flows into a Nernst-Planck equation and coupled it with the volume fraction advection equation, momentum balance equation with the electrohydrodynamic force, continuity equation, Gauss's law along with the electrostatic approximation and solved the resulting system of equations to simulate the transport of cations in a drop. We observed the breakup of a two-dimensional drop due to the addition of ions with unbalanced charge. In this article,

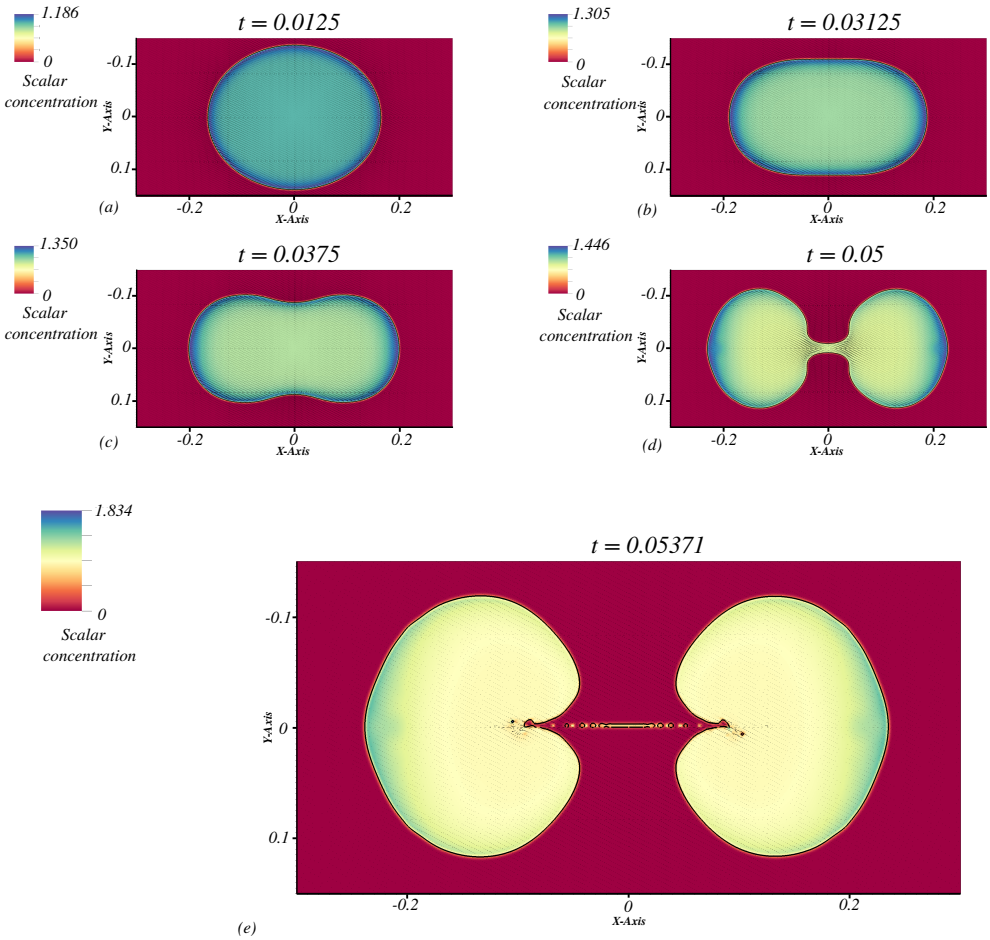


FIGURE 10. Time evolution of the breakup of a perturbed drop due to the addition of ions with unbalanced charge.

results are presented for one and two-dimensional domains. However, it is straightforward to extend this to three dimensions, and the results for these are deferred to a future article.

## Acknowledgments

This investigation was funded by Office of Naval Research, Grant No. N00014-19-1-2425. S. S. Jain was also supported by the Franklin P. and Caroline M. Johnson Fellowship. The authors would like to thank Parviz Moin and Shahab Mirjalili for fruitful discussions on diffuse-interface method, and Ronald Chan for reviewing this article.

## REFERENCES

BERRY, J., DAVIDSON, M. & HARVIE, D. J. 2013 A multiphase electrokinetic flow model for electrolytes with liquid/liquid interfaces. *J. Comput. Phys.* **251**, 209–222.

CRAIG, V., NINHAM, B. & PASHLEY, R. 1993 Effect of electrolytes on bubble coalescence. *Nature* **364**, 317.

Fernandez, D., Maurer, P., Martine, M., Coey, J. & Mobius, M. E. 2014 Bubble formation at a gas-evolving microelectrode. *Langmuir* **30**, 13065–13074.

Griffiths, D. J. 2005 *Introduction to electrodynamics*. Cambridge University Press.

Jain, S. S., Mani, A. & Moin, P. 2019 A conservative diffuse-interface method for compressible two-phase flows. *arXiv preprint arXiv:1911.03619* .

Kataoka, I. 1986 Local instant formulation of two-phase flow. *Int. J. Multiphas. Flow* **12**, 745–758.

Kim, J. & Moin, P. 1985 Application of a fractional-step method to incompressible Navier-Stokes equations. *J. Comput. Phys.* **59**, 308–323.

Kirby, B. J. 2010 *Micro-and nanoscale fluid mechanics: transport in microfluidic devices*. Cambridge University Press.

Laney, C. B. 1998 *Computational gasdynamics*. Cambridge University Press.

Mirjalili, S., Ivey, C. B. & Mani, A. 2019 Comparison between the diffuse interface and volume of fluid methods for simulating two-phase flows. *Int. J. Multiphas. Flow* **116**, 221–238.

Mirjalili, S., Ivey, C. B. & Mani, A. 2020 A conservative diffuse interface method for two-phase flows with provable boundedness properties. *J. Comput. Phys.* **401**, 109006.

Mirjalili, S., Jain, S. S. & Dodd, M. 2017 Interface-capturing methods for two-phase flows: An overview and recent developments. *Annual Research Briefs*, Center for Turbulence Research, Stanford University, pp. 117–135.

Mittal, R. & Moin, P. 1997 Suitability of upwind-biased finite difference schemes for large-eddy simulation of turbulent flows. *AIAA J.* **35**, 1415–1417.

Moin, P. & Verzicco, R. 2016 On the suitability of second-order accurate discretizations for turbulent flow simulations. *Eur. J. Mech. B-Fluid.* **55**, 242–245.

Patankar, S. 1980 *Numerical heat transfer and fluid flow*. CRC press.

Saville, D. 1997 Electrohydrodynamics: the Taylor-Melcher leaky dielectric model. *Annu. Rev. Fluid Mech.* **29**, 27–64.

Versteeg, H. K. & Malalasekera, W. 2007 *An introduction to computational fluid dynamics: the finite volume method*. Pearson Education.

Wasekar, V. & Manglik, R. 2000 Pool boiling heat transfer in aqueous solutions of an anionic surfactant. *J. Heat Transf.* **122**, 708–715.